

A Novel Method for Detection of Wind Turbine Blade Imbalance Based on Multi-Variable Spectrum Imaging and Convolutional Neural Network

Zhe Cao¹, Jian Xu², Wei Xiao¹, Yanjing Gao¹, Haotian Wu²

1. State Key Laboratory of Fluid Power Transmission and Control, Zhejiang University, Hangzhou 310027, P. R. China

2. College of Electrical Engineering, Zhejiang University, Hangzhou 310027, P. R. China

E-mail: 11725040@zju.edu.cn

Abstract: This paper presents a novel method used for detecting blade imbalance occurring on wind turbines based on multi-variable spectrum imaging and convolutional neural network (CNN). The balance and imbalance conditions were simulated with the aid of commercial wind turbine design software Bladed. Simulation results including generator speed, generator torque and nacelle X acceleration were obtained and processed with Fourier transform to generate the combined spectral images, which were then fed to a CNN model in order to extract and learn the fault features. The effectiveness of the proposed method was validated through comparison with single variable CNN and fully-connected neural network. Results demonstrate that this method is capable of detecting aerodynamic imbalance and mass imbalance with high accuracy and high efficiency.

Key Words: blade imbalance, wind turbine, convolutional neural network, power spectrum

1 Introduction

Wind power is a renewable and sustainable energy source that gains high popularity in the background of limited amount of traditional energy sources and massive pollution generated by the combustion of fossil fuel. In the year 2017, the total wind power generation capacity in mainland China has increased by 11.7%, reached 188 GW [1].

Wind turbines are usually installed on high towers in some remote regions or even offshore [2]. Therefore, it is crucial to reduce maintenance efforts as well as downtime for the sake of high electricity output. Blade imbalance is one of the most common faults in wind turbines, especially in large-scale wind turbines with long blades. It can be a consequence of aerodynamic asymmetry, pitch angle misalignment, inhomogenous mass distribution in the blade due to manufacturing defects, fatigue, icing and dust soaking, which are usually observed in harsh operating environment [3]. Blade imbalance will potentially result in vibrations in blades and drivetrain, causing severe power loss, and moreover, aggravate the fatigue and damage the whole turbine [2, 3].

Various methods have been proposed for early detection of the blade imbalance, most of which use certain techniques to extract the fault features contained in vibration signal, generator current or other variables. For instance, [2–8] used various approaches including derivation, Hilbert envelope demodulation, dq coordinate transformation, order tracking analysis, etc. to analyse the stator current or rotor current in frequency domain, which can enhance the fault features while diminishing the influence of fundamental frequency. [9] analysed the aerodynamic torque signal measured on the hub and used order tracking method to extract the characteristic frequency of blade angle faults. [10] clearly explained the differences between aerodynamic imbalance and rotor mass imbalance. They managed to distinguish one from each other by different harmonics in rotor speed frequency spectrum. However, the result was merely validated under steady wind conditions. Some researchers also studied the relation-

ship between blade imbalance and the vibration of the wind turbine by conducting finite element analysis [11] or developing a numerical model [12].

On the other hand, as the concepts of deep learning and artificial intelligence start to flourish in recent years, several intelligent algorithms with machine learning techniques have been applied on the fault diagnosis of mechanical components including gearbox, bearing, etc. [13–16]. However, such applications are rarely found in wind turbine blade imbalance detection. For example, [17] used neural networks to analyse the harmonics of the rotor response and identify cause, severity and location of the imbalance. However, further details about simulation environment and training process were not included. In [18–20], researchers adopted various techniques including fuzzy Q learning, artificial neural networks, gene expression programming, empirical mode decomposition, principal component analysis and decision tree to extract and identify the fault characteristics from the generator current signals generated by a combined simulation environment implemented with TurbSim, FAST and Simulink. [21] proposed a diagnosis method combining the modified sparse autoencoder and softmax regression to process the images of marine current turbine taken by camera and detect the imbalance induced by additional weight attached to one of the blades.

Compared to traditional machine learning algorithms, convolutional neural network (CNN) has the capability of automatically extracting features from original data without the requirement of expertise knowledge or cumbersome pre-processing. Once the model is trained, the identification process only takes less than one second to complete.

In this study, CNN was adopted to extract and learn the fault features from the frequency spectral data generated from simulations, which were conducted under time-varying wind conditions. Result proved that the proposed method is capable of accurately identifying different aerodynamic imbalances and mass imbalances with high efficiency under different turbulent wind flows.

2 Convolutional Neural Network

Convolutional neural network (CNN) is a class of deep neural network inspired by the biological processes of visual perception. Since the early 2000s, CNN has been applied to the detection, segmentation and recognition of objects and regions in images with great success. It is designed to process the data in the form of multiple arrays [22]:

- 1D: signals, language or other time sequences.
- 2D: images, audio spectrograms.
- 3D: volumetric images (e.g. MRI), videos.

Compared to fully-connected neural networks or other traditional machine learning algorithms, CNN has the following advantages: automatic feature extraction, strong expression ability enhanced with its deep structure and nonlinearity, several techniques to overcome overfitting including pooling layer, dropout layer, weight decay, and moreover, less parameters to optimise because of shared weights.

Fig. 1 shows the architecture of a typical CNN. CNN consists of a series of stages, which usually starts with convolutional layers and pooling layers [22]. The final stages are largely similar to a multilayer perceptron neural network, consisting of fully-connected layers and a classifier.

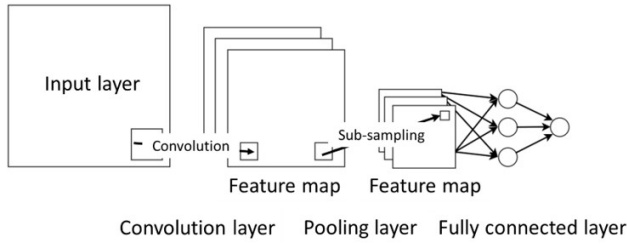


Fig. 1: Architecture of a typical CNN

A convolutional layer contains a set of filters, w , also known as kernels or receptive fields, which conduct convolutions on the input layer x . Each filter contains the weights shared by all the input neurons and reproduces a feature map through a certain type of activation function f , e.g. ReLU (rectified linear unit). The entirety of the extracted feature maps forms the input data of the next layer y , which can be expressed as:

$$y = f(\sum w * x + b) \quad (1)$$

where b denotes bias [15]. The convolution process to some extents emulates the response of neurons to external visual stimuli. The function of convolutional layers is to extract features automatically from input data.

A pooling layer usually follows a convolutional layer, using sub-sampling to obtain a lower resolution of the feature maps. The most common one is max pooling, which keeps the maximum value of each cluster of neurons at the feature maps. Pooling layers can significantly reduce the computational effort and prevent overfitting.

After a series of convolutional layers and pooling layers, the output neurons in the form of multiple-dimensional array are flattened as a 1-D array and fed to fully-connected layers (also known as dense layers), where all the neurons from two adjacent layers are completely interconnected. The outputs of fully-connected layers can be represented as the outputs

of multilayer perceptrons:

$$y = f(\sum x * w + b) \quad (2)$$

where x are the inputs from the previous layer, w and b denote weights and bias, respectively. f denotes the activation function, e.g. ReLU, or softmax, if y is the final output.

Softmax function is currently one of the most commonly used classifiers in CNN. Mathematically, softmax function converts an unnormalised vector into a normalised probability distribution. The predicted probability of the j th class is represented as:

$$P(y = j|x; w_j, b_j) = \frac{e^{x*w_j+b_j}}{\sum_{k=1}^K e^{x*w_k+b_k}} \quad (3)$$

where K is the dimension of the output.

Once the structure and all the hyperparameters are set, the network is ready to be trained. The performance of CNN is evaluated against the ground truth by a predefined loss function, e.g. root mean square and categorical cross entropy. The training objective is to optimise the loss function on all learnable parameters, i.e. w and b . CNN is usually trained with backpropagation method, which computes the loss function as well as the gradient that is required for optimisation from the output and distributes backwards through layers. To save computational effort, normally in each epoch, the loss function is calculated on a subset of the training samples (known as batch) rather than all of them.

3 Blade Imbalance Simulation

Commercial wind turbine design software Bladed was used to simulate the operation of a 2.0 MW wind turbine. Bladed is built with rigorous engineering model and validated thoroughly against turbine measurements, it has been the wind power industry standard for over 20 years. The wind turbine parameters used in the simulation are listed in Table 1. In this study, two types of blade imbalance were investigated: aerodynamic imbalance, induced by deliberately changing one of the three pitch angles; mass imbalance, induced by attaching imbalance mass on the blades.

Table 1: Parameters of a 2.0 MW wind turbine

Rated power	2.0 MW
Rotor diameter	115 m
Tower height	78 m
Cut-in wind speed	3 m/s
Cut-out wind speed	20 m/s
Rated generator speed	1800 rpm

The simulations were conducted under 9 sets of turbulent wind flows with the average wind speeds ranging from 4, 6, 8, ..., 20 m/s. For aerodynamic imbalance, the pitch angles were ranged from 1° to 4° every 0.5° . The magnitude of mass imbalance was evaluated by the imbalance ratio, defined by the imbalance torque divided by the aerodynamic torque. In this simulation, the imbalance ratio was ranged from 1% to 5%. Each simulation was conducted over a time period of 330 seconds.

Fig. 2 shows the examples of time history data including generator speed, generator torque, nacelle X acceleration (denoting vibration in swaying direction) with three different

wind flows under the same aerodynamic imbalance condition. It is obvious that each variable varies greatly in time domain as a consequence of unsteady wind flow despite a decreasing trend in variability observed at higher wind speeds

due to the active pitch-regulated control. It is not advisable to identify the fault patterns directly from time domain data since their trends are largely dependent on wind speed.

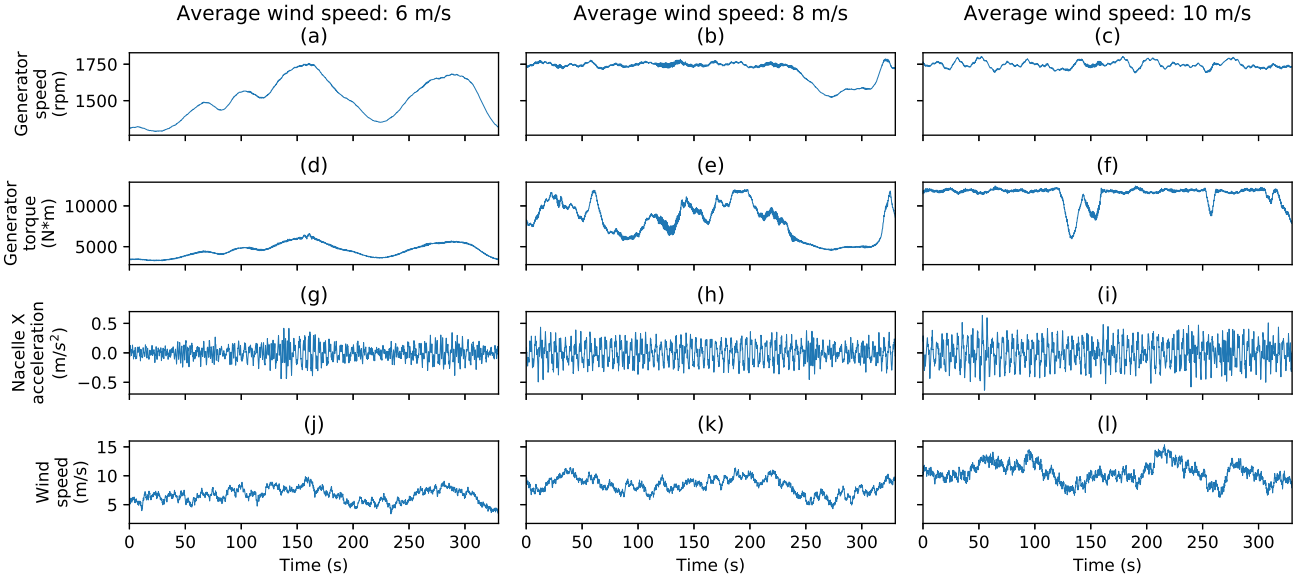


Fig. 2: Time history of generator speed, generator torque, nacelle X acceleration and wind speed under an aerodynamic imbalance condition (one of the pitch angles deliberately changed to 4°) with wind flows of average speed = 6 m/s: (a), (d), (g), (j); 8 m/s: (b), (e), (h), (k); 10 m/s: (c), (f), (i), (l)

One of the intuitive solutions is using Fourier transform to obtain the frequency components in the signals. Fig. 3 shows the power spectrum of the generator speed signal under balance, aerodynamic imbalance and mass imbalance conditions with wind flow remaining unchanged. It can be observed that energy are mainly concentrated on low frequencies and there are only slight differences between each power spectrum, which means the noise, fluctuations and other factors might be prone to affect the fault features. Hence, these features in frequency data could be recognised and extracted by CNN. And hopefully, through abundant amount of data, CNN can successfully learn the patterns of aerodynamic imbalance and mass imbalance in frequency data regardless of time-varying wind flows and the severity of imbalances,

4 Experiments and Discussions

4.1 Data Description

Further analysis on the power spectrum indicates that different types of imbalance source have different patterns and trends when average wind speed or output variable is changed. For example, mass imbalance tends to be more distinguishable at lower wind speeds, whereas aerodynamic imbalance is more distinguishable at higher wind speeds; and that aerodynamic imbalance differs from balanced condition much more than mass imbalance does in terms of the power spectrum of nacelle X acceleration. For the sake of brevity, details are not shown here.

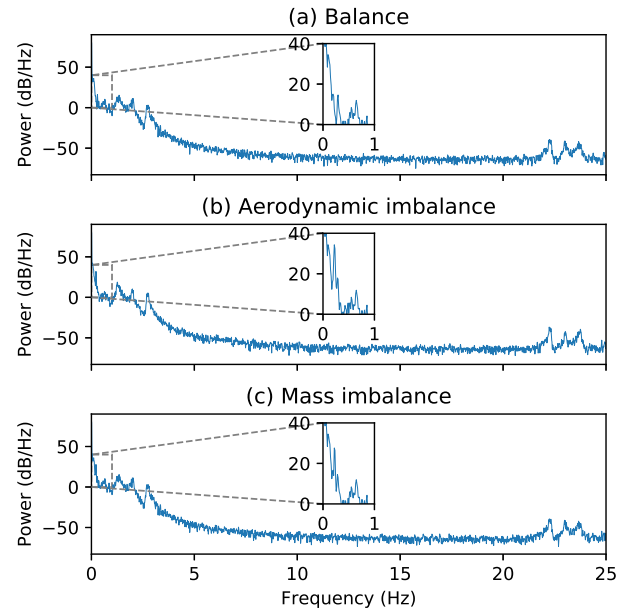


Fig. 3: Power spectrum of generator speed under: (a) balanced; (b) aerodynamic imbalance; (c) mass imbalance conditions with the same wind flow of average wind speed = 14 m/s

Therefore, in order to improve the accuracy of the detection and the overall performance of the model, a novel data pre-processing method was proposed. For each piece of time domain data, the power spectra of three signals: namely generator speed, generator torque and nacelle X accelera-

tion, were generated and combined together. Concretely, each spectrum contains a series of the same length: 2048, of which only the first 256 values were kept since prior analysis indicates that fault features mainly concentrate on lower frequencies; the value series were scaled among all the samples to the range of (0, 1); 3 series were stacked to a normalised spectral image of 3×256 . In this way, each sample will contain the frequency data of three variables. CNN will make predictions on the basis of the characteristics of three power spectra rather than only one, which in turn reduces the random error and improves the reliability of the results.

From the aforementioned simulations, a data set consisting of 837 samples was generated, including 378 aerodynamic imbalance samples, 216 mass imbalance samples and 243 balanced samples. The data set was randomly split into training set, validation set and test set, each containing 576, 131 and 130 samples. Fig. 4 shows some examples of samples of each category in grayscale images.

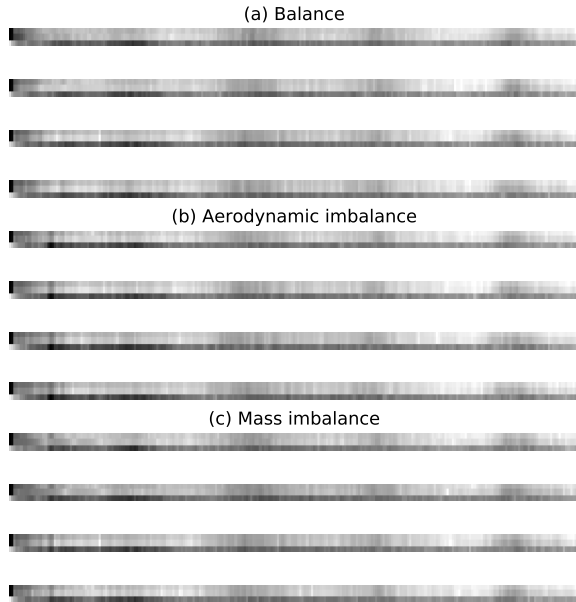


Fig. 4: Examples of spectral images of (a) balance; (b) aerodynamic imbalance and (c) mass imbalance samples

4.2 CNN Design

The structure of the CNN proposed in this study is shown in Fig. 5. The input data is a 1-channel 3×256 array. The input layer is followed by two sets of convolutional + pool-

ing layers. The first convolutional layer consists of 16 1×7 kernels with 1×3 strides; the second convolutional layer consists of 32 1×5 kernels with 1×2 strides. Both pooling layers use 1×2 max pooling. After the above operations, the features map is unrolled as a 1D array and fed to fully-connected layers for classification. Two hidden layers were used, each containing 128 and 30 neurons. The output layer has 3 neurons since it is a three category classification problem (balance; aerodynamic imbalance; mass imbalance). Trials and errors proved that the parameters as listed in Table. 2 could achieve high accuracy while significantly simplifying the model and reducing training time.

Table 2: Parameters of the CNN

Layer	Output shape	Activation function
Input	(3, 256, 1)	–
2D convolution	(3, 86, 16)	ReLU
Max pooling	(3, 43, 16)	–
2D convolution	(3, 22, 32)	ReLU
Max pooling	(3, 11, 32)	–
Flatten	1056	–
Dense	128	ReLU
Dense	30	ReLU
Dense	3	Softmax

Optimiser	RMSprop
Loss function	Categorical cross entropy
Learning rate	0.0003
Batch size	32

4.3 Results and Analysis

Fig. 6 shows the learning curves of the model from epoch 1 to 300. It can be observed that loss function converges to zero and that the model achieves 100% accuracy as training continues. The entire training process including data conversion completes in less than 20 seconds. The confusion matrix in Fig. 7 demonstrates the prediction result in a clearer way. It indicates that all samples in each category were correctly predicted and that there is no misdetection.

To demonstrate the effectiveness of multi-variable spectrum imaging, the 1D CNN model using only one variable out of three was also trained. Fig. 8 shows the learning curves of the 1D CNN model. It is obvious that the result is highly oscillatory and that the loss is much higher, which indicates that the result is less reliable. Compared to 1D CNN model, the proposed model has significantly higher convergence rate and accuracy.

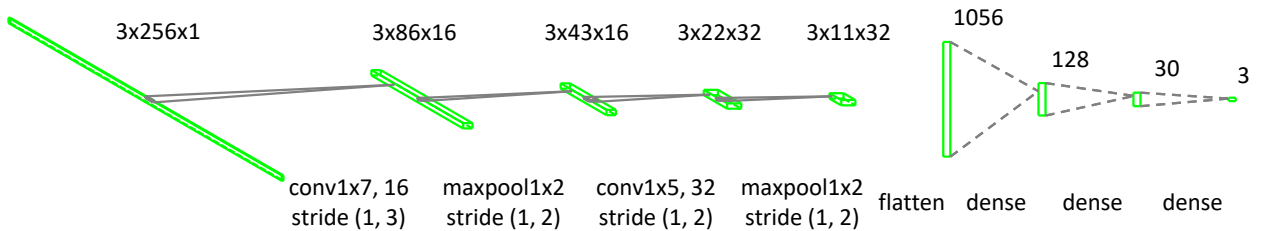


Fig. 5: CNN architecture

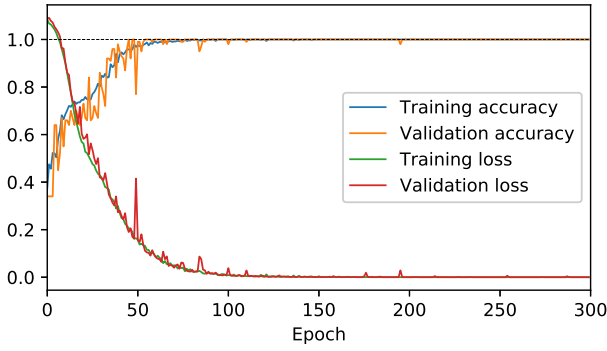


Fig. 6: Learning curves of multi-variable CNN model

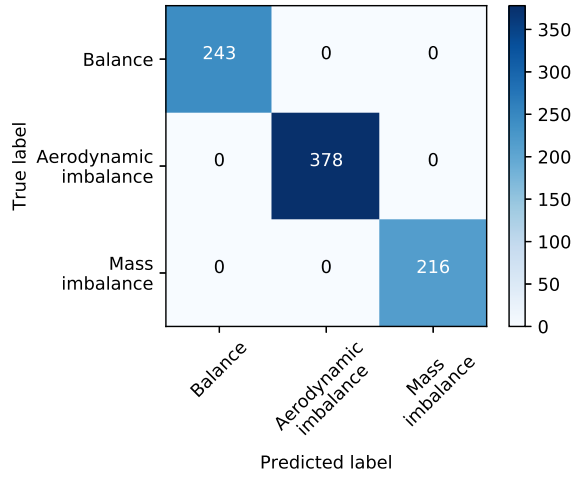


Fig. 7: Confusion matrix

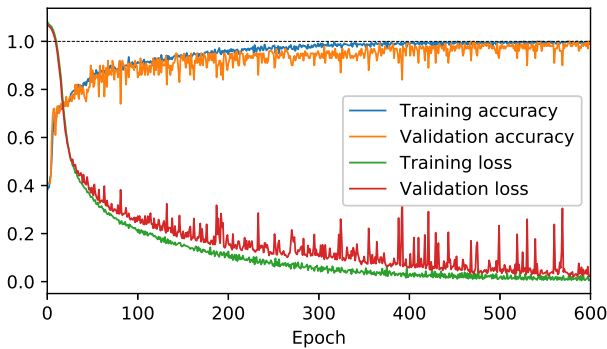


Fig. 8: Learning curves of single variable 1D CNN model

Table.3 lists the accuracy of the proposed CNN model on test set based on 10 trials, in comparison with the results of 1D CNN and fully-connected neural network (denoted as ANN). Therefore, it can be proved that the method presented here has great advantages over the one variable CNN and fully-connected neural network. The feature extraction characteristics of CNN remarkably increase both accuracy and training speed. It has smaller model size compared to traditional ANN owing to its shared weights. Moreover, using multi-variable as the input data has largely augmented the in-

formation contained in the input data and helped to produce more reliable results.

Table 3: Comparison of average testing accuracy between different models

Model	Multi-variable CNN	1D CNN	ANN
Testing accuracy	100%	97.8%	94.0%

5 Conclusion

In this study, a novel method for wind turbine blade imbalance detection was presented. The wind turbine operations under balance, aerodynamic imbalance and mass imbalance conditions in time-varying turbulent wind flows were simulated in Bladed. The power spectra of the generated signals including generator speed, generator torque and nacelle X acceleration were combined into a 2D spectral image. A CNN model including two sets of convolutional + pooling layers was then proposed to extract the fault features contained in the spectral images and detect the imbalance fault. The performance of the proposed method was compared with fully-connected neural network and the CNN using only one variable. Result demonstrated that this method can quickly detect aerodynamic imbalance and mass imbalance with 100% accuracy regardless of the time-varying characteristics of the output signals. Future work will be focused on the validation of the method through experimental data and the implementation of the online balancing monitoring system.

References

- [1] Wind Power Branch of China Association of Agricultural Machinery Manufacturers, China wind energy industry annual report 2017-2018.
- [2] J. Qiu, G. Xu, J. Tao and J. Yang, Study on detection of blade imbalance for DFIG WTS based on spectrum analysis of Hilbert modulus, *Journal of Engineering*, 2017(13): 1338–1342, 2017.
- [3] L. Shi, J. Qiu, G. Xu, J. Yang and J. Wang, Online detection for blade imbalance of doubly fed induction generator wind turbines based on stator current, *The 2nd International Conference on Power and Renewable Energy*, 2017: 428–433.
- [4] H. Li, D. Yang, C. Yang, Y. Hu, Z. Liu and Y. Lan, Blade imbalance fault diagnosis of doubly fed wind turbines based on stator current feature analysis, *Automation of Electric Power Systems*, 39(13): 32–37, 2015.
- [5] G. Xiang and Q. Wei, Imbalance fault detection of direct-drive wind turbine using generator current signals, *IEEE Transactions on Energy Conversion*, 27(2): 468–476, 2012.
- [6] Y. Li, X. Sheng, S. Wan and L. Cheng, Blade mass imbalance fault diagnosis using rotor and stator current based on coordinate transformation and HED, *IEEE 8th International Power Electronics and Motion Control Conference*, 2016: 987–992.
- [7] X. Sheng, S. Wan, Y. Li and L. Cheng, Fault diagnosis for blade mass imbalance of wind turbines with DFIG based on coordinate transformation, *Transactions of China Electrotechnical Society*, 31(7): 188–197, 2016.
- [8] X. Sheng, S. Wan, L. Cheng and Y. Li, Wind turbines blade asymmetry fault diagnosis based on rotor current, *Computer Simulation*, 35(6): 106–109, 407, 2018.
- [9] P. Li, W. Hu, J. Liu and Z. Chen, Using order tracking analysis method to detect the angle faults of blades on wind turbine, *Proceedings of the 35th Chinese Control Conference*, 2016: 6801–6806.

- [10] M. Shahriar, P. Borghesani and A. Tan, Speed-based diagnostics of aerodynamic and mass imbalance in large wind turbines, *2015 IEEE International Conference on Advanced Intelligent Mechatronics*, 2015: 796–801.
- [11] S. Zhang, W. Zhang, K. Wang and Y. Chen, The impact of unbalance mass caused by installment error of the blades on the vibration of the wind turbine tower, *Machine Design & Manufacture*, 2009(9): 140–142, 2009.
- [12] J. Niebsch, R. Ramlau and T. Nguyen, Mass and aerodynamic imbalance estimates of wind turbines, *Energies*, 2010(3): 696–710, 2010.
- [13] L. Jing, M. Zhao, P. Li and X. Xu, A convolutional neural network based feature learning and fault diagnosis for the condition monitoring of gearbox, *Measurement*, 111(2017): 1–10, 2017.
- [14] M. Amar, I. Gondal and C. Wilson, Vibration spectrum imaging: A novel bearing fault classification approach, *IEEE Transactions on Industrial Electronics*, 62(1): 494–501, 2015.
- [15] J. Li and W. Qu, Aero-engine sensor fault diagnosis based on convolutional neural network, *Proceedings of the 37th Chinese Control Conference*, 2018: 6049–6054.
- [16] R. Sánchez, P. Lucero, J. Macancela, M. Cerrada, R. Vázquez and F. Pacheco, Multi-fault diagnosis of rotating machinery by using feature ranking methods and SVM-based classifiers, *International Conference on Sensing, Diagnosis, Prognostics and Control*, 2017: 105–110.
- [17] S. Cacciola, I. Agud and C. Bottasso, Detection of rotor imbalance, including root cause, severity and location, *Journal of Physics: Conference Series*, 753 072003, 2016.
- [18] H. Malik and S. Mishra, Application of fuzzy Q learning (FQL) technique to wind turbine imbalance fault identification using generator current signals, *2016 IEEE 7th Power India International Conference*, 2016: 1–6.
- [19] H. Malik and S. Mishra, Artificial neural network and empirical mode decomposition based imbalance fault diagnosis of wind turbine using TurbSim, FAST and Simulink, *IET Renewable Power Generation*, 11(6): 889–902, 2017.
- [20] H. Malik and S. Mishra, Application of GEP to investigate the imbalance faults in direct-drive wind turbine using generator current signals, *IET Renewable Power Generation*, 12(3): 279–291, 2018.
- [21] P. Wen, T. Wang, B. Xin, T. Tang and Y. Wang, Blade imbalanced fault diagnosis for marine current turbine based on sparse autoencoder and softmax regression, *The 33rd Academic Annual Conference of Chinese Association of Automation*, 2018: 246–251.
- [22] Y. LeCun, Y. Bengio and G. Hinton, Deep learning, *Nature*, 521: 436–444, 2015.